Design and Experimental Verification of a 3D Magnetic EZ Antenna at 300 MHz

Richard W. Ziolkowski, *Fellow, IEEE*, Chia-Ching Lin, *Student Member, IEEE*, Jean A. Nielsen, Minas H. Tanielian, and Christopher L. Holloway, *Senior Member, IEEE*

***Abstract*—Several variations of a 300-MHz version of the electrically small coax-fed three-dimensional (3D) magnetic EZ antenna were designed and tested. The final version of this low-profile antenna had an electrical size that was $ka \sim 0.437$ at 300.96 MHz. Nearly complete matching to the 50-Ω source and high overall efficiency (nearly 100%) were achieved. The measured fractional bandwidth was approximately 1.66%. The numerically predicted and the measured results were in good agreement. Comparisons to similar-sized loop antennas that were matched to the source with both custom-made and commercially available, general purpose external matching networks confirm the performance enhancements achieved with this metamaterial-inspired, near-field resonant parasitic antenna.**

***Index Terms*—Antenna theory, electrically small antennas, metamaterials, parasitics, quality factors.**

I. Introduction

AN EFFICIENT, electrically small antenna design methodology has been presented previously in [1]–[4]. The main innovation of those designs was the introduction of an electrically small metamaterial-inspired parasitic element in the very near-field of the electrically small radiator. "Inspired" refers to the fact that the parasitic element could be used as the unit cell inclusion in a conventional metamaterial. The metamaterial-inspired parasitic structure facilitates the antenna system being resonant (reactive matching) and resistively matched to the source (50 Ω), without any external matching network. If a is the radius of the smallest enclosing sphere and $k = 2\pi/\lambda_{\rm res}$, where $\lambda_{\rm res}$ is the free-space wavelength corresponding to the resonance frequency $f_{\rm res} = c/\lambda_{\rm res}$, it was demonstrated experimentally [4] that the overall efficiency of a two-dimensional (2D) electric EZ antenna with $f_{\rm res} = 1.37$ GHz and $ka \sim 0.49$ was ∼94%, with a 4.1% fractional bandwidth. S-parameters were also measured for two 2D magnetic EZ antennas in the 430-MHz range. However, no three-dimensional (3D) cases were fabricated and tested. As reported in [5], it was desirable to move the 3D magnetic EZ antennas to lower frequencies for several applications. In this letter, we report the design, fabrication, and testing of several versions of the 3D magnetic EZ antenna at 300 MHz. These types of metamaterial-inspired antennas help overcome the loss issues associated with an actual metamaterial-based antenna design [6].

Manuscript received July 27, 2009. First published August 11, 2009; current version published September 15, 2009. This work was supported in part by DARPA Contract HR0011-05-C-0068. Part of this effort was U.S. government work, not subject to U.S. copyright.

R. W. Ziolkowski and C.-C. Lin are with the Department of Electrical and Computer Engineering, University of Arizona, Tucson, AZ 85721-0104 USA (e-mail: ziolkowski@ece.arizona.edu).

J. A. Nielsen and M. H. Tanielian are with Boeing Research & Technology, Seattle, WA 98124-2499 USA.

C. L. Holloway is with the Electromagnetics Division, National Institute of Standards and Technology (NIST), Boulder, CO 80305 USA.

Color versions of one or more of the figures in this letter are available online at http://ieeexplore.ieee.org.

Digital Object Identifier 10.1109/LAWP.2009.2029708

II. Initial Designs and Measurements

The near-field resonant parasitic element of the 3D magnetic EZ antennas [2], [4] is an extruded capacitively loaded loop (CLL). It is driven by a semiloop antenna coaxially fed through a ground plane. As shown in [2]–[4], the resonance frequency of these EZ antennas is given by the expression

$$f_{\rm res} = \frac{1}{2\pi\sqrt{L_{\rm eff}C_{\rm eff}}} \tag{1}$$

where $L_{\rm eff}$ and $C_{\rm eff}$ are the effective inductance and capacitance of the system. Consequently, one can adjust $f_{\rm res}$ simply by changing either of these effective values. For instance, the effective capacitance of the CLL element can be tuned by changing the dimensions of its capacitive gap or the permittivity in this gap region. All of the designs reported here used a quartz slab in the gap region. Quartz was selected because it is a very low-loss dielectric at the frequencies of interest and has $\varepsilon_r = 3.78$. This higher-than-vacuum relative permittivity value lowered $f_{\rm res}$ for a given CLL element size and, hence, allowed us to consider parasitic elements that were smaller than in previous vacuum-based designs to achieve the same effective capacitance.

A 3D magnetic EZ antenna was designed for operation at approximately 300 MHz using Ansoft HFSS (mention of this product is not an endorsement, but only serves to clarify the software used). The baseline design size had right-angled corners and its size (length × width × height) was $80 \times 80 \times 40$ mm^3. To fabricate it, a coaxial, panel mount connector was attached to the back of a circular copper plate that was ultimately inserted into a larger ground plane so that the dielectric was flush with the front surface. Then, a copper wire was bent to form the loop; and the ends were soldered into the connector and a corresponding hole drilled into the insert. The bent sections of the antenna were formed by cutting copper sheets to the correct dimensions and then bending them to form the corners; they were mechanically stabilized by cutting slots through the ground plane insert and sliding the vertical sections into those holes. Subsequently, these sections were laser-welded into place from the back of the insert. When the CLL pieces are laser-welded to the circular plate, the resulting bending can change the gap size. Placing the quartz slab into the connective gap of the CLL element helps maintain this critical dimension, i.e., the quartz slab also provides

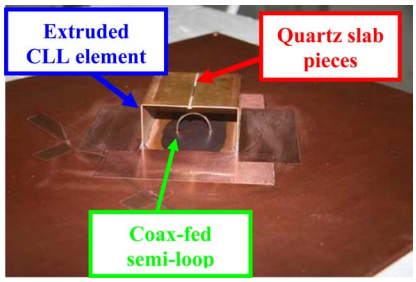

Fig. 1. Fabricated 3D magnetic EZ antenna integrated into its large ground plane. The CLL capacitive gap is partially filled with quartz slabs.

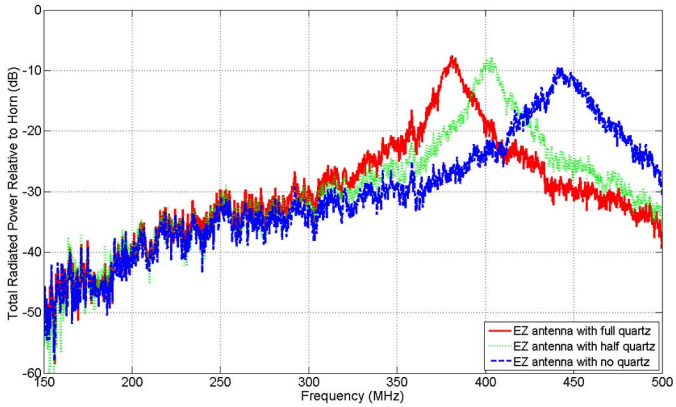

Fig. 2. Measured total radiated power relative to the reference horn for three different amounts of quartz in the capacitive gap of the CLL element.

structural (mechanical) stability. The quartz was attached with a low-loss adhesive.

The S-parameters and power efficiency of the fabricated antennas were measured in the reverberation chambers at the National Institute of Standards and Technology (NIST) in Boulder, CO. Reverberation chambers (RCs) have become increasingly popular as an alternative test facility for a wide variety of electromagnetic measurements [7], [8]. While pattern measurements are unavailable, RCs are nonetheless ideal environments for measuring the total radiated power and efficiency of an antenna [8]–[11]. Furthermore, the RC approach to measure the radiation efficiency of an antenna has been demonstrated to be a reliable alternative to the traditional Wheeler Cap and anechoic chamber methods [9]–[11]. All radiated power measurements reported here were made relative to a reference antenna, an ETS-LINDGREN_model 3106 dual-ridged waveguide horn that is about 94% efficient in its 200 MHz–2 GHz frequency band. The reverberation chamber was $2.8 \times 3.1 \times 4.6$ m^3 in size for the antenna characterization. This NIST chamber used two rotating paddles in order to reduce the uncertainties in the measurements to 1.0 dB or less [12].

The fabricated EZ antenna in its large ground plane configuration is shown in Fig. 1. Note that, as fabricated, the antenna has a small (120.6-mm diameter copper plate) ground plane. It is then inserted into a larger (18 in $\times$ 18 in $=$ 457.2 mm $\times$ 457.2 mm) copper ground plane (or not), as shown in Fig. 1, for measurement. To verify the efficacy of using the quartz slab as a tuning element, the antenna was measured in three configurations: no slab, half of the slab, and full slab. The measured relative total radiated power results for these configurations are shown in Fig. 2. Three basic results can be inferred from these initial measurements. The resonance frequency of the EZ antenna was tunable by the amount of quartz in the capacitive gap of its CLL element. The total radiated power was enhanced near the resonance frequency of the CLL element. The resonance frequencies were far from the predicted value of 300 MHz.

Careful examination of the fabricated parasitic led us to further analyze the design through a series of parametric studies with HFSS. It was found that the rounded corners, particularly in the capacitive gap, have a very significant impact on the resonance frequency, i.e., they have a dramatic effect on the capacitance produced by the dielectric-filled gap. This rounding of the corners occurs during the bending of the copper. The antenna was thus redesigned to account for the rounded corners.

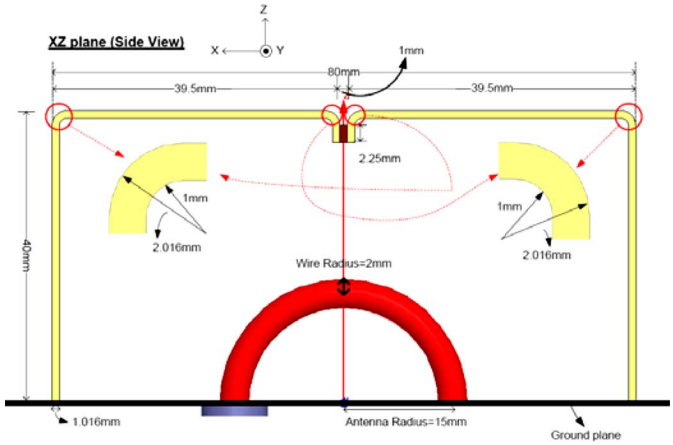

Fig. 3. Final design of the rounded-corner, 3D magnetic EZ antenna.

III. Final Design and Measurements

The final design (in cross-sectional view) and its dimensions are shown in Fig. 3. The length, width, and height of the CLL element remained, respectively, at 80, 80, and 40 mm. This is a low-profile design, i.e., its height is only $\lambda_{\rm res}/25$. The fabricated final design is shown in Fig. 4. All predicted values agree reasonably well with the measured values. The predicted resonance frequency was $f_{\rm res} = 300.77$ MHz, giving $ka = 0.437$; i.e., $a \sim \lambda_{\rm res}/15$. The antenna is electrically small at the design frequency. The HFSS-predicted value of the overall efficiency (total radiated power to total input power) was 99%. The predicted fractional bandwidth (FBW), based on the half-power VSWR bandwidth, was 1.83%. This means the Q value was 7.43 times the Chu limit [13] and 2.48 times the (magnetic-based antenna) Thal limit [14].

The measured relative total radiated power of the EZ antenna as a function of the frequency, when it was placed on the wall and in the center of the reverberation chamber, is given in Fig. 5. In the former antenna-under-test (AUT) configuration, the measured $f_{\rm res} = 309.8$ MHz, where $\rm S_{11} = -22.40$ dB, and $\rm FBW = 1.29\%$. In the latter, the measured $f_{\rm res} = 297.75$ MHz, where $\rm S_{11} = -30.73$ dB, and $\rm FBW = 1.36\%$. The slight differences in the observed resonance frequencies are due to the different AUT measurement setups. The center-of-the-chamber

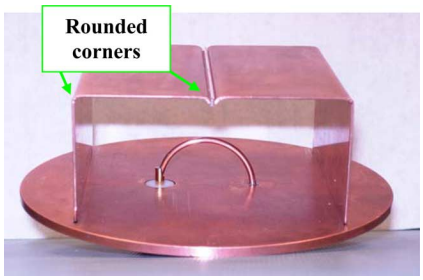

Fig. 4. The fabricated 3D magnetic EZ antenna with its small ground plane. As constructed, the extruded CLL element has all rounded corners.

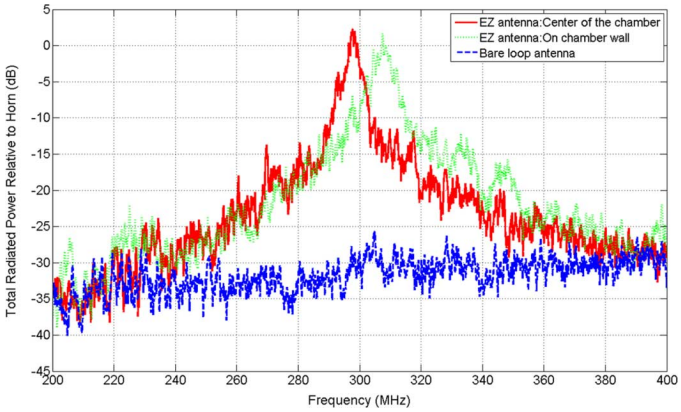

Fig. 5. Comparison of the measured relative total radiated power of the 3D magnetic EZ antenna and the bare loop antenna.

AUT configuration measurements were also performed with several other cable layouts to confirm that the cable was not contributing to the measured total radiated power. These included loading the cable with a variety of ferrite beads at numerous different cable locations. The chamber wall measurements eliminated this issue since the cable was located in its exterior. Both AUT configurations yielded similar results; they both demonstrated that the EZ antenna is radiating more efficiently than the reference horn. The observed fractional bandwidth was smaller than predicted; the FBW values were obtained from the average of many measurement samples. A separate stand-alone vector-network analyzer (VNA) measurement gave $\mathrm{FBW} = 1.77\%$, in much better agreement with the HFSS-predicted value.

Results for the bare semiloop antenna placed in the center-of-the-chamber AUT configuration are also given in Fig. 5. The HFSS-predicted input impedance of the bare 15.0-mm radius semiloop antenna at 300.77 MHz was $0.03 + 44.38\ \mathrm{j}\ \Omega$. This corresponds to a -28.7-dB value for the accepted power for the 50-Ω feedline. The measured relative total radiated power of the bare semiloop is approximately -30 dB. Consequently, agreement between all of the simulation and experimental results was obtained. This particular comparison was performed to confirm that, as predicted, the metamaterial-inspired near-field resonant parasitic acts as an internal matching network, which produces nearly complete matching to the source, and enhances the total radiated power by acting as a transducer, which changes the reactive field of the driven element into a propagating field.

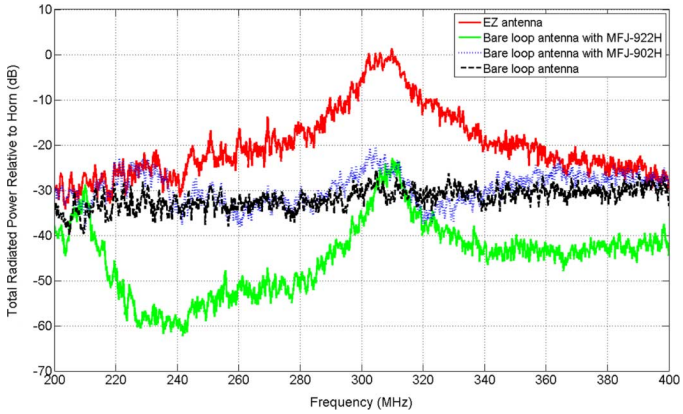

Fig. 6. Comparison of the measured relative total radiated power of the 3D magnetic EZ antenna, the bare loop antenna, and two external matching network augmented semiloop antennas.

We also tested the bare semiloop with two different kinds of external matching network devices. They were an MFJ-902H Travel Tuner and an MFJ-922 VHF/UHF dual-band antenna tuner. It was expected that these comparison cases would further confirm that the near-field resonant parasitic provided more than just an internal matching network. In both instances, measured S_{11} values below -30 dB were obtained between 300 and 310 MHz. A comparison of the relative total radiated power measured as a function of the frequency for the EZ antenna and the corresponding bare semiloop in the center-of-the-chamber AUT configuration is shown in Fig. 6. The peaks of the MFJ-902H and the MFJ-922 total radiated power results were -20.61 dB at 304.55 MHz and -22.9148 dB at 309.95 MHz, respectively. Thus, the matched semiloop values were more than 20 dB smaller than the EZ antenna results. Again, these measurements were confirmed with several alternate ferrite bead-loaded cable configurations.

Additional simulations were conducted with several coax-based stub tuner external matching networks, and similar very low total radiated powers were obtained. They indicated that the bare semiloop is so electrically small that the resistive loss in the copper is significantly larger than the radiation loss. However, because the losses could have been caused simply by the component losses in the MFJ tuners, we proceeded to retest these results using a single stub tuner of our own design. These measurements provided additional comparisons between the various EZ antenna configurations and a well-matched semiloop antenna. They were taken in the new $2.95 \times 3.63 \times 4.27\ \mathrm{m}^3$ reverberation chamber at NIST.

We thus designed, fabricated, and tested a single stub tuner that matched the 15.0-mm semiloop antenna to the assumed 50-Ω source. The stub of the tuner was offset from the antenna terminals by 388.41 mm, and the coaxial stub itself had a length equal to 260.37 mm. Taking into account the copper losses in the antenna and the coax lines, the HFSS-predicted values were: radiation efficiency $\mathrm{RE} = 1.9\%$ (-17.21 dB) with $\mathrm{S}_{11} = -33.3$ dB at 299.715 MHz and, thus, a -17.48 dB relative total radiated power value. While the radius of the semiloop gives $ka = 0.094$ at that frequency, including the matching network for a fair size comparison then yields $ka = 1.51, 3.46$

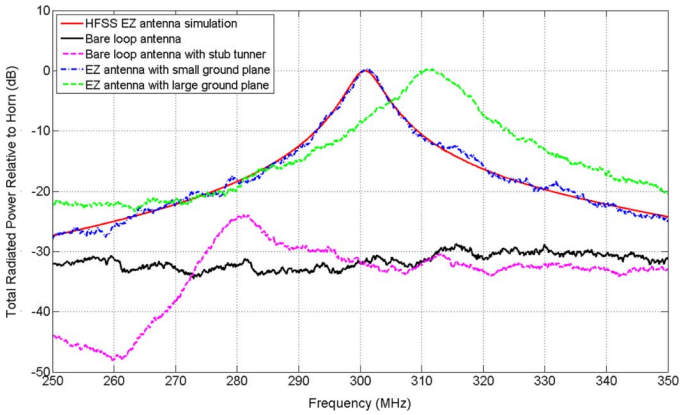

Fig. 7. Comparison of the predicted and measured (new NIST reverberation chamber) relative total radiated power of the EZ antenna with the small ground plane and with the large ground plane, the bare semiloop antenna, and the stub-tuner matched semiloop antenna.

times larger than the EZ antenna value. The physically tested tuner had a stub length that was 220 mm; it was inserted into the feedline about 420 mm from the end of the coax. This design was obtained by experimentally testing the S_{11} values and adjusting the cable length until matching was obtained. The S_{11} value was measured to be approximately -47 dB at 320 MHz. The overall system was not electrically small at that frequency, i.e., including the stub tuner, $ka \sim 1.63$, making it about 3.74 times larger than the EZ antenna.

A comparison of the total radiated power measured as a function of the frequency in the center-of-the-chamber AUT configuration for the EZ antenna with the large ground plane, the EZ antenna with the small ground plane, and the corresponding HFSS simulation results are shown in Fig. 7. Also included are the corresponding results for the bare semiloop antenna and for the stub-tuner-matched semiloop antenna. The resonance of the small (large) ground plane version of the EZ antenna occurred at $f_{\mathrm{res}} = 300.96$ MHz (311.78 MHz) with $ka = 0.437$ (0.453) and $\mathrm{FBW} = 1.66\%$ (2.83%). The stub-tuner results were consistent with the MFJ tuner results. We believe that the extra stub length and the multiple pieces of coax needed to create the stub caused the relative total radiated power value to be lower than the HFSS-predicted values. Consequently, the EZ antenna was measured to be about 30 dB more efficient than the matched semiloop antenna and is slightly more efficient than the reference horn antenna at the design frequency. These experimental results again confirm that the near-field resonant parasitic of the EZ antenna leads to both nearly complete matching to the source and to an improved radiation efficiency.

Further comparisons were made numerically by redesigning the HFSS model to be a rectangular semiloop wire antenna having the same dimensions as the cross section of the extruded CLL element, i.e., 40 mm $\times$ 80 mm, and a 2.0-mm wire diameter. The HFSS-predicted input impedance of this much larger semiloop antenna was $\mathrm{Z}_{\mathrm{in}} = 2.65 + \mathrm{j}360.06\,\Omega$ at 300.77 MHz. The coax stub-tuner designed to match this antenna to the assumed 50-Ω source was offset from the antenna terminals by 281.29 mm and had a length equal to 239.37 mm. The HFSS-predicted values for the resulting single-stub tuned semiloop antenna were $\mathrm{RE} = 9.68\%$ (-10.14 dB) with $\mathrm{S}_{11} = -31.8$ dB at 300.94 MHz, giving -10.41 dB as the relative total radiated power value. Accounting for the additional losses encountered in the other tuner comparison cases (either the general purpose commercial box or the fabricated design), this value would be even lower in practice. Thus, even if the physical size of the semiloop antenna were comparable to the parasitic, the EZ antenna would still have more than a ten-times larger relative total radiated power value even though it is 2.89 times smaller electrically, i.e., while the minimum enclosing radius of the rectangular semiloop alone gives $ka = 0.357$, including the associated matching network then yields $ka = 1.26$.

IV. Conclusion

We have demonstrated that the electrically small, metamaterial-inspired, 3D magnetic EZ antenna, which consists of a directly driven semiloop antenna, coaxially fed through a finite ground plane, and a near-field resonant parasitic element (an extruded capacitively loaded loop), performs as predicted at 300 MHz. Several versions were designed, fabricated, and tested. The final designs took into account the actual fabrication nuances to achieve good agreement between the simulated and measured results. Nearly complete matching with no external matching circuit for a ($ka = 0.437$)-sized EZ antenna was demonstrated at 300.96 MHz with a fractional bandwidth of 1.66%. Reverberation chamber measurements of its total radiated power demonstrated a greater than 95% overall efficiency at that resonance frequency. Direct comparisons with a comparable semiloop antenna with several different external matching networks also demonstrated that the 3D magnetic EZ antenna was significantly more efficient than any of the electrically larger, externally matched semiloop antennas. We are continuing our investigations to determine whether such near-field resonant parasitic antennas can operate at even lower (VHF) frequencies. A 100-MHz 3D magnetic EZ antenna has been designed and fabricated and is currently being evaluated.

References

[1] R. W. Ziolkowski and A. Erentok, "Metamaterial-based efficient electrically small antennas," *IEEE Trans. Antennas Propag.*, vol. 54, no. 7, pp. 2113–2130, Jul. 2006.

[2] A. Erentok and R. W. Ziolkowski, "An efficient metamaterial-inspired electrically-small antenna," *Microw. Opt. Tech. Lett.*, vol. 49, no. 6, pp. 1287–1290, Jun. 2007.

[3] A. Erentok and R. W. Ziolkowski, "Two-dimensional efficient metamaterial-inspired electrically-small antenna," *Microw. Opt. Tech. Lett.*, vol. 49, no. 7, pp. 1669–1673, Jul. 2007.

[4] A. Erentok and R. W. Ziolkowski, "Metamaterial-inspired efficient electrically-small antennas," *IEEE Trans. Antennas Propag.*, vol. 56, no. 3, pp. 691–707, Mar. 2008.

[5] R. W. Ziolkowski and C.-C. Lin, "Metamaterial-inspired magnetic-based UHF and VHF antennas," in *Proc. 2008 IEEE AP-S Int. Symp. USNC/URSI Nat. Radio Sci. Meeting*, San Diego, CA, Jul. 5–12, 2008, paper no. 207.3.

[6] R. B. Greegor, C. G. Parazzoli, D. C. Vier, S. Schultz, C. L. Holloway, and R. W. Ziolkowski, "Demonstration of impedance matching using a mu-negative (MNG) metamaterial," *IEEE Antennas Wireless Propag. Lett.*, vol. 8, pp. 92–95, 2009.

[7] P. Wilson, G. Koepke, J. Ladbury, and C. L. Holloway, "Emission and immunity standards: Replacing field-at-a-distance measurements with total-radiated-power measurements," in *Proc. IEEE Int. Symp. Electromagn. Compat.*, Montreal, Canada, Aug. 13–17, 2001, vol. 2, pp. 964–969.

[8] C. L. Holloway, D. A. Hill, J. M. Ladbury, P. Wilson, G. Koepke, and J. Coder, "On the use of reverberation chambers to simulate a controllable Rician radio environment for the testing of wireless devices," *IEEE Trans. Antennas Propag.*, vol. 54, no. 11, pp. 3167–3177, Nov. 2006.

[9] N. Serafimov, P.-S. Kildal, and T. Bolin, "Comparison between radiation efficiencies of phone antennas and radiated power of mobile phones measured in anechoic chambers and reverberation chamber," in *Proc. IEEE Antennas Propag. Int. Symp.*, San Antonio, TX, Jun. 16–21, 2002, vol. 2, pp. 478–481.

[10] A. A. H. Azremi, H. G. Shiraz, and P. S. Hall, "Small antenna efficiency by the reverberation chamber and the Wheeler cap methods," in *Proc. 13th IEEE Int. Conf. Netw.*, Kuala Lumpur, Malaysia, Nov. 16–18, 2005, pp. 12–16.

[11] G. Le Fur, C. Lemoine, P. Besnier, and A. Sharaiha, "Performances of UWB Wheeler cap and reverberation chamber to carry out efficiency measurements of narrow band antennas," *Antennas Wireless Propag. Lett.*, vol. 8, pp. 332–335, 2009.

[12] D. A. Hill and M. Kanda, "Measurement uncertainty of radiated emission," Boulder, CO, 1997, NIST Tech. Note 1389.

[13] L. J. Chu, "Physical limitations of omni-directional antennas," *J. Appl. Phys.*, pp. 1163–1175, 1948.

[14] H. Thal, "New radiation Q limits for spherical wire antennas," *IEEE Trans. Antennas Propag.*, vol. 54, no. 10, pp. 2757–2763, Oct. 2006.